frontiers in Earth Science

ORIGINAL RESEARCH
published: 28 May 2021
doi: 10.3389/feart.2021.672119

Hints on the Late Miocene Evolution of the Tonale-Adamello-Brenta Region (Alps, Italy) Based on Allochtonous Sediments From Raponzolo Cave

Francesco Sauro[1], *Maria Giuditta Fellin*[2], *Andrea Columbu*[1]*, *Philipp Häuselmann*[3], *Andrea Borsato*[4], *Cristina Carbone*[5] *and Jo De Waele*[1]

[1]Department of Biological, Geological and Environmental Sciences, University of Bologna, Bologna, Italy, [2]Geological Institute, ETH Zürich, Zürich, Switzerland, [3]Swiss Institute for Speleology and Karst Studies (SISKA), La Chaux-de-Fonds, Switzerland, [4]School of Environmental and Life Sciences, University of Newcastle, Callaghan, NSW, Australia, [5]Department of Earth, Environmental and Life Sciences (DISTAV), Genoa University, Genoa, Italy

OPEN ACCESS

Edited by:
Andrea Zerboni,
University of Milan, Italy

Reviewed by:
Nadja Zupan Hajna,
Research Center of the Slovenian Academy of Sciences and Arts, Slovenia
Fabio Matano,
National Research Council, Italy
Fabrizio Berra,
University of Milan, Italy

***Correspondence:**
Andrea Columbu
andrea.columbu@unibo.it

Specialty section:
This article was submitted to Quaternary Science, Geomorphology and Paleoenvironment, a section of the journal Frontiers in Earth Science

Received: *25 February 2021*
Accepted: *10 May 2021*
Published: *28 May 2021*

Citation:
Sauro F, Fellin MG, Columbu A, Häuselmann P, Borsato A, Carbone C and De Waele J (2021) Hints on the Late Miocene Evolution of the Tonale-Adamello-Brenta Region (Alps, Italy) Based on Allochtonous Sediments From Raponzolo Cave. Front. Earth Sci. 9:672119. doi: 10.3389/feart.2021.672119

Raponzolo is a paleo-phreatic cave explored in 2011 in the Brenta Dolomites (Trentino, Italy), at the remarkable altitude of 2,560 m a.s.l. Differently to all other caves of the area, it hosts well-cemented fine to medium sands of granitic-metamorphic composition. The composition suggests a sediment source from the Adamello and Tonale Unit, separated from the Brenta by one of the most important tectonic lineaments of the Alps (Giudicarie Line). The fine-sand sediment was sampled to determine burial time and thus a minimum age of the cave. Cosmogenic isotopes (^{26}Al and ^{10}Be) in quartz grains allowed to estimate a minimum burial age of 5.25 Ma based on the mean sediment transport time at the surface and infer original altitude of the catchment area. Detrital apatite fission-track (AFT) and U-Pb dating on zircons provide information on the source, both from a regional and altitude (exhumation) perspective. Two populations of detrital AFT ages center at 17 (–2.3 + 2.6) Ma and 23 (–3.3 + 3.9) Ma, whereas the main detrital zircon U-Pb age populations are younger than 40 Ma. These correspond to intrusive and metamorphic sources nowadays outcropping exclusively above 2,200–2,300 m a.s.l. in Northern Adamello and Tonale. The results point to a late Miocene erosion and infilling of the cave by allochtonous sediments, with important implications on the timing of cave speleogenesis, as well as the paleogeographical connection, tectonic evolution and uplift of different structural units of the Alps. The roundness and the well sorted size of the quartz grains suggest a fluvial or aeolian origin, possibly recycled by glacial activity related to cold events reported in high latitude areas of the world at 5.75 and 5.51 Ma. These glacial phases have never been documented before in the Alps. This information confirms that the valleys dividing these geological units were not yet deeply entrenched during the onset of the Messinian Salinity Crisis (5.6–5.5 Ma), allowing an efficient transport of sediments across major tectonic lineaments of the Alps. This study shows the potential of cave sediments to provide information not only on the age of speleogenesis but also on the paleogeography of a wide area of the Alps during the late Miocene.

Keywords: Al-Be isotopes, speleogenesis, paleogeography, cave sediments, AFT analysis, U-Pb zircon dating

INTRODUCTION

Understanding how the topography and physiography of the Alps evolved from the Eocene to the Miocene has been one of the main challenges in Alpine geology over the last decades (Schmid et al., 2004; Garzanti and Malusà, 2008; Schlunegger and Mosar, 2011; Campani et al., 2012; Winterberg and Willett, 2019). Paleogeographic reconstructions based on synorogenic detrital archives have resolved large-scale features of the surface evolution of the Alps (Carrapa and Di Giulio, 2001; Kuhlemann and Kempf, 2002). A detailed exhumation history of the metamorphic and igneous rocks of the Alps has been reconstructed based on a dense thermochronologic dataset (Fox et al., 2016). However, carbonate massifs as those of the Southern Alps are difficult to integrate into paleogeographic and exhumation/uplift models, lacking powerful chronological, thermal and distinct compositional markers applicable to these geological terrains. While the evolution of the Southern Alps has been studied through structural mapping and tectonic reconstruction (Doglioni and Bosellini, 1987; Castellarin and Cantelli, 2000), scarce information is available on the absolute timing of the events, uplift, erosion rates and especially paleogeographic arrangements in pre-Quaternary times (Stefani et al., 2007; Malusà et al., 2009; Potter and Szatmari 2009; Fox et al., 2016). This information gap could be fulfilled by the study of karst system, which are abundant in the Southern Alps. Kartsic caves are often characterized by the presence of well-developed paleo-phreatic levels evolving in response to surface evolution and valley entrenchment (Audra et al., 2007; Sauro et al., 2012). The arrangement of these cave levels can be correlated with the deepening of the water table due to uplift of karst massifs through time; however, constraining speleogenetic phases with absolute chronology remains challenging (Sauro et al., 2013; Columbu et al., 2015; Columbu et al., 2017; Ballesteros et al., 2019; Bella et al., 2019). The study of allochthonous sediments in ancient cave systems can be a powerful tool to better understand the paleogeographic evolution in karst areas (Stock et al., 2005b). While calcite speleothems can grow at any (usually air-filled) stage once the void is formed, and are mainly useful for paleoclimatic and paleo-environmental reconstructions (Fairchild et al., 2006), the introduction of allochthonous sediments within cave systems is often synchronous or occurs shortly after the genesis of cave passages (Häuselmann, 2007; Calvet et al., 2015), i.e., when the base level is still more or less at the same altitude of the caves themselves (Columbu et al., 2018). In this case, burial time corresponds to the approximate age of the phreatic karst network at specific water table levels (Granger et al., 2001; Häuselmann and Granger, 2005). Accordingly, cosmogenic dating on cave sediments has been successfully applied in the North-Western calcareous Alps (Häuselmann and Granger, 2005), in the Eastern Austrian Alps (Häuselmann et al., 2020), in the Southern calcareous Alps of Slovenia (Häuselmann et al., 2015) and in other karst areas of the World (Anthony and Granger, 2007; De Waele et al., 2012; Calvet et al., 2015; Granger et al., 2015; Columbu et al., 2021). Nonetheless, a set of conditions has to be satisfied to consider a cave as a potential site for sediment burial studies and to meaningfully link cave development to tectonic evolution: 1) The presence of quartz-rich terrains in the vicinity of the karst system, procuring the sediment source; 2) geological and environmental conditions able to transport these allogenic sediments from the source area to the karstified units; 3) the injection of the sediment into the phreatic or epiphreatic conduits, often developed close to the local water table. In addition, the sediment should not be re-eroded, moved and stored in younger conduits at lower levels without having been exposed at the surface again. If this later transport would happen the age obtained with cosmogenic dating could not be associated to the correct speleogenetic phase (Häuselmann et al., 2020).

The Brenta Dolomites Massif is one of the areas of the Southern Alps where information about uplift and tectonic evolution is scarce. This area is situated to the south-east of a crucial tectonic triple junction (Doglioni and Bosellini, 1987), at the intersection between the Periadriatic line and the Giudicarie South and North lines (**Figures 1**, **2**), close to the border between the Austroalpine and Southern Alps (Heberer et al., 2017).

The Brenta Dolomites Massif represents the northern area of a mainly carbonatic mountain chain region of the Southern Alps, within the Giudicarie tectonic Belt. Permian volcano-sedimentary deposits are exposed in a few outcrops in the valley entrenchment of the Giudicarie South line (between Rendena Valley and Sabion Line, **Figure 2**), but the most widespread formation in the Brenta Massif is the Upper Triassic "Dolomia Principale" (blue in **Figure 2**), a carbonate shelf succession made up of a ~1,000 m thick sequence of massive and laminated dolostones (Borsato et al., 1994; Carton and Baroni, 2017). The Brenta Massif is characterized by a well-developed karst landscape with several deep vadose vertical caves and some subterranean networks presenting paleophreatic morphologies (Conci and Galvagni, 1952; Borsato, 1991; Borsato et al., 2003; Audra et al., 2006). This makes the Brenta Massif one of the most important karst areas in the Dolomites, with a well-articulate subsurface drainage network discharging in large karst springs along its perimeter at elevations between 1,400–1,600 m a.s.l. (perched aquifers) and 400–600 m a.s.l. (base level springs) (Borsato, 2001; Borsato, 2007). The Brenta karst area is bordered by metamorphic and intrusive units. Indeed, to the north-west, the region is characterized by the metamorphic nappes of Tonale, formed by high pressure mineral assemblages (Stipp et al., 2002; Spalla et al., 2003).To the west there is the Adamello Batholith, one of the most investigated areas of the Alps (Brack 1983; Martin et al., 1993; Fellin et al., 2002). Adamello is mostly composed of igneous rocks belonging to a large batholith formed by tonalite, granodiorite and gabbro (Callegari and Brack, 2002). It is the largest intrusive body of Alpine Tertiary magmatism emplaced during the Eocene to the early Oligocene. Adamello and Brenta both exhumed from 2 to 3 km depth relatively to the modern surface since the late Miocene (Reverman et al., 2012; Heberer et al., 2017; Stalder et al., 2018). Both Adamello and Tonale are now separated from Brenta Massif by deep glacial valleys entrenched along the main tectonic lines (**Figure 1**).

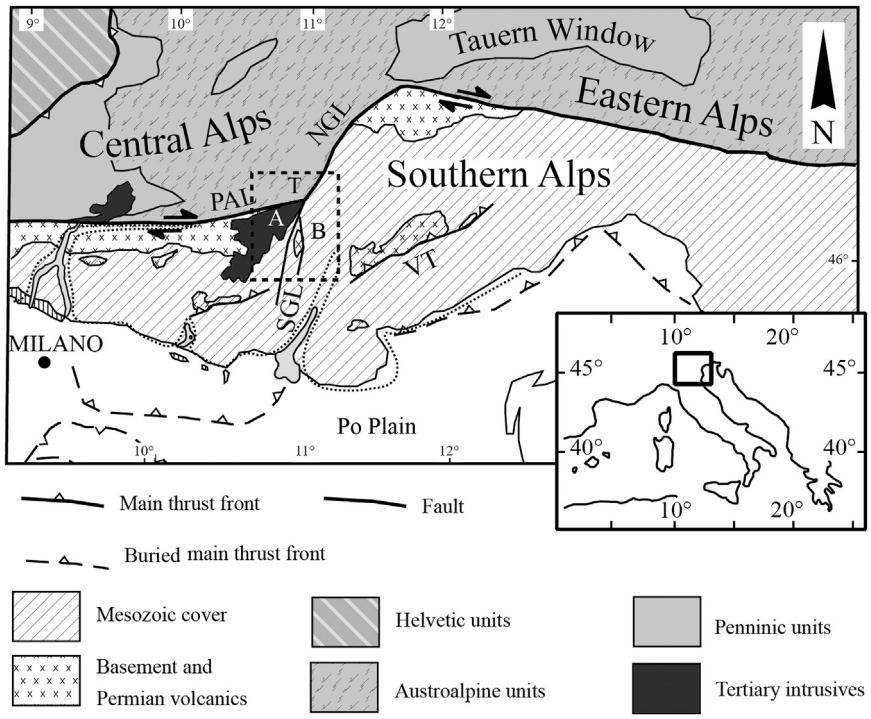

FIGURE 1 | Geographic overview of the Adamello (A), Brenta (B), Tonale (T) massifs in the frame of the Southern and Central Alps. The dotted box is approximately the area of **Figure 2**. (Modified from Reverman et al., 2012). PAL = Periadriatic Line; NGL = Northern Giudicarie Line; SGL = Southern Giudicarie Line; VT = Valsugana Thrust.

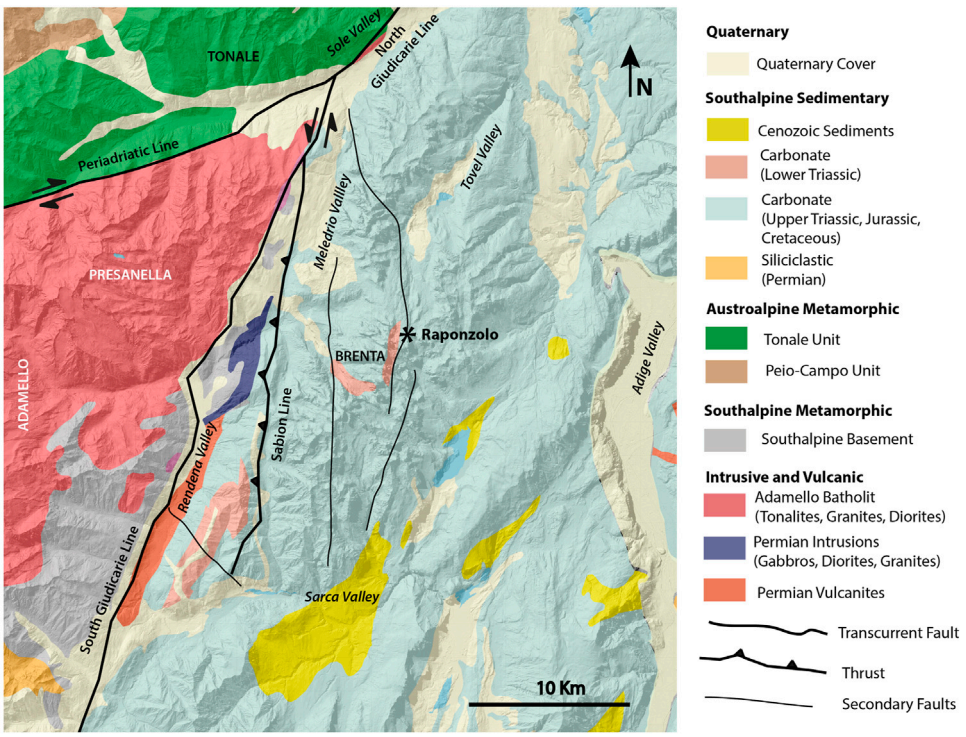

FIGURE 2 | Regional geology of the study area and location of Raponzolo Cave (simplified from Bigi and Carrozzo, 1992).

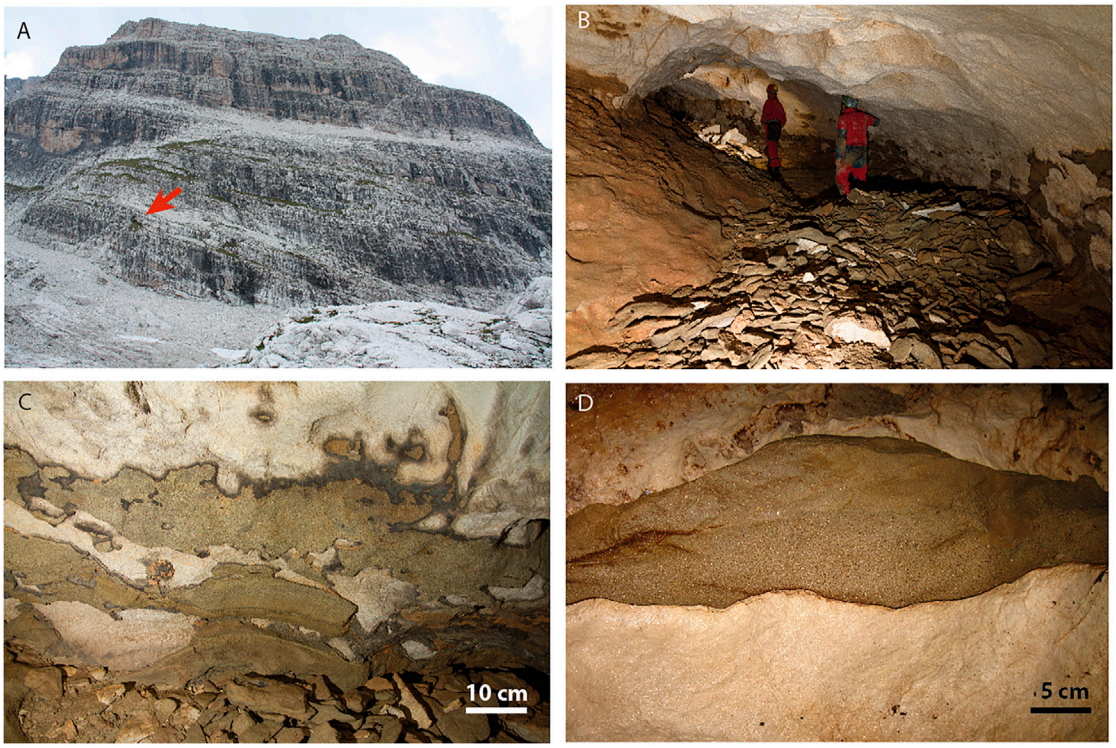

FIGURE 3 | Cave morphologies and sediment: **(A)** The entrance of the Cave is a gallery truncated by erosion on the cliffs of Cima Grosté (red arrow); **(B)** Typical paleophreatic conduit with elliptical shape and big scallops due to phreatic slow flow; **(C)** Remnants of cemented sandstone sediments on cave walls; **(D)** A sedimentary fracture infilling on the cave roof indicating that the whole gallery was originally filled and then re-excavated.

Until a few decades ago, the caves of the Brenta Massif were considered mostly related to the last glacial phases (Nicod, 1976); the discovery of extensive phreatic galleries at 2,100 m a.s.l., 1,300 m above the present-day local groundwater table (Borsato, 1991; Borsato, 2012), suggested that speleogenetic processes were indeed more ancient and complex. In fact, several U/Th dating of speleothems from the Brenta Massif as well as on the nearby Paganella mountain are in secular equilibrium for $^{238}U/^{234}U$ isotopes attesting an age older than 1 Ma (Bini et al., 1991; Borsato et al., 2003; Audra et al., 2007). However, no evidence of allochthonous cave sediments were known in the Brenta Massif until 2011, when the Gruppo Speleologico Trentino SAT Bindesi Villazzano discovered Raponzolo Cave, which represents a portion of a paleo-phreatic gallery of a presumably pre-Quaternary karst system given the high altitude occurrence (2,560 m asl). The main cave passage was partially filled with allochthonous sandy sediments mainly composed of quartz and biotite. This discovery opened the possibility of performing sediment source and burial age studies in the area for the very first time. Consequently, the study of ancient Brenta karst systems and sediments trapped within cave conduits could represent a key for understanding the evolution of this massif.

This paper shows how a detailed analysis of cave sediments can provide valuable information on the geological and speleogenetic history of a cave, providing new hints on the paleogeography and tectonic evolution of a wide region of the Alps.

AREA OF STUDY, MATERIALS AND METHODS

The Raponzolo Cave

Raponzolo Cave opens at 2,560 m asl (46°11′55.1″N, 10°54′40.7″E), on the steep eastern flank of Cima Grosté (2,898 m a.s.l.), toward the upper end of the Tovel Valley, the widest valley of the Brenta Massif (3.5 km of width, **Figure 2**). The cave is a single sub-horizontal tunnel about 180 m long, excavated in the Dolomia Principale formation. An initial W-trending ascending gallery paved with loose dolomitic sand is followed by a N-trending descending gallery partially filled with cemented medium-fine siliciclastic sand (**Figures 3**, **4**). Comparable sediments are not found anywhere else in the area. The sediments are present on the gallery floor as well as on walls and roofs, suggesting that the whole conduit was once filled (and then re-excavated). The cave presents typical phreatic morphologies with large scallops up to 0.5 m in diameter, without traces of vadose morphologies (**Figure 3B**).

The analyses targeted pristine and well cemented sediment samples from Raponzolo Cave. A multi-technique approach was used to obtain information about composition, provenance and

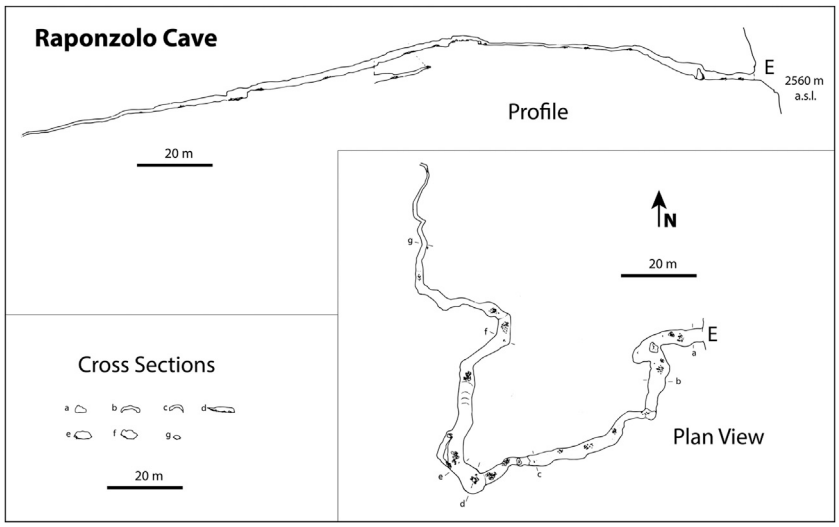

FIGURE 4 | Topographic map of Raponzolo Cave (survey GST-SAT BV).

burial time. These included: petrographic observation using an optical microscope, X-Ray Diffraction (XRD), X-Ray Fluorescence (XRF), ^{26}Al and ^{10}Be cosmogenic isotopes, Apatite Fission Track (AFT) analyses and U-Pb dating on zircons.

Petrographic Observations and Grainsize

Petrographic observations were accomplished on three thin sections (~25 μm) with a LEICA Stereomicroscope and an OLYMPUS BX-41 optical microscope. Images have been obtained using a OLYMPUS COLOR VIEW II-SET camera and processed through OLYMPUS C-VIEW II-BUND-cellB software. For grainsize measurements, 300 g of sample have been treated with a 70% acetic acid solution in order to dissolve the carbonate cement and release the insoluble fraction for grain size measurements through sieves. Pre- and post-dissolution weighing ascertained the cement/sediment ratio. Grainsize measurement utilized standard ASTM sieves 25, 40, 70, 100, 200, 230 and >230, with meshes corresponding to 0.71, 0.425, 0.212, 0.15, 0.075, 0.063 and <0.063 mm, respectively. Analyses were accomplished at Bologna University (Italy).

XRF and XRD Analysis

The sample was ground to ultrafine powders and kept 24 h at 110°C. Ten grams of sample were mixed with 2.5–5 ml of Elvacite polymer resin, dissolved in acetone. The mixture was stirred to allow acetone evaporation and Elvacite distribution. The resultant powder was placed in a penny-shaped mold and compressed with a vertical pressure of 40 MPa for 1 min. A WD-XRF Axios–Panalytical spectrometer equipped with five diffraction crystals was used for the analyses. The SuperQ software package provided by Panalytical was employed for calibration and data reduction. Calibration is based on 30 certified international standards. The precision of analyzed elemental abundances is better than ± 0.2% for SiO_2, and ± 0.1% for the other major elements except for MnO_2 and P_2O_5 that have concentration errors of approximately ± 0.02%. For trace elements, relative errors are up to 10% for concentrations of 10–100 ppm, better than 5% for higher concentrations and reaching ~50% at levels below 10 ppm. Therefore, the detection limit is approximately 5–10 ppm.

The mineralogical composition was investigated by a Philips PW3710 X-Ray diffractometer (current: 20 mA, voltage: 40 kV, range 2θ: 5–80°, step size: 0.02° 2θ, time per step: 2 s) operating at the University of Genua (Italy), which mounted a Co-anode. Acquisition and processing of data was carried out using the Philips High Score software package.

Cosmogenic Isotopes

The burial age method involves the measurement of two isotopes (^{26}Al and ^{10}Be) that are produced by cosmic radiation in quartz near the surface prior to burial. ^{26}Al and ^{10}Be accumulate at a ratio of about 6.8:1 (Balco et al., 2013) in quartz grains, with a rate of a few atoms per Gram of quartz per year. Sufficiently deep burial (more than 10 m) of such quartz-rich sediments in a cave assures shielding from further cosmic rays. After burial, the ^{26}Al and ^{10}Be concentrations in the sample are only affected by their relative decay resulting in a decrease in the ^{26}Al/^{10}Be ratio. This ratio can be used to derive a burial age (Gosse and Phillips, 2001; Granger, 2006). A prerequisite of the burial dating technique is that samples have been exposed long enough to cosmic rays and accumulated sufficient cosmogenic nuclides prior to burial. The upper limit for measurement of the ^{26}Al and ^{10}Be isotope pair is between 5 and 6 Ma depending on the accumulated cosmogenic isotopes during surface exposure (Häuselmann et al., 2020).

The isotope concentrations can also be used to infer paleo-erosion rates of the source area prior to burial of the clasts. This is accomplished by backward modeling the quantity of nuclides present prior to the burial coupled with local production rate estimates. The pre-burial ^{26}Al/^{10}Be ratio (~6.8:1) is basically not influenced by production rate and thus elevation (Nishiizumi et al., 1989; Stock et al., 2005a) and therefore burial ages remain unaffected by altitude changes in the source area.

The sediment sample was broken into smaller pieces and decarbonated using HCl; due to many accessory minerals, only

38.0062 g of pure quartz could be recovered. Quartz was sieved and the fraction between 250 and 710 μm was physically concentrated (separation by form, magnet- and reverse magnet separation and heavy liquid) and then cleaned with HF-HNO_3 to remove intergrown feldspars to obtain a clean quartz concentrate. This concentrate was dissolved and cleaned by dissolution, precipitation, and ion exchange. ^{26}Al and ^{10}Be were separated, precipitated, oxidized, and measured on an AMS (in Purdue University). Chemical blanks were also measured to subtract laboratory influence. The AMS measures the $^{10}Be/^{9}Be$ ratio and the $^{26}Al/^{27}Al$ ratio; while ^{9}Be is added artificially, ^{27}Al normally abounds in quartz-rich samples.

Apatite Fission-Track Analyses

Fission-tracks in apatite are damage zones in the crystal lattice formed during the radioactive decay of ^{238}U. At temperatures above 120°C tracks are quickly annealed, whereas at temperatures below 60°C tracks are retained. The temperature range between retention and total annealing is called the partial annealing zone (PAZ). In this range fission tracks progressively narrow and shorten as a function of time and temperature (Naeser, 1979).

Fission-track sample preparation and analysis were performed on 100 apatite grains at ETH Zurich. Mounts of grains were polished and etched in 5.5 N HNO_3 at 21°C for 20 s to reveal spontaneous tracks. Samples were irradiated with thermal neutrons in the reactor at the Radiation Center of Oregon State University with a nominal fluence of 1.2×10^{16} n/cm^2. The CN-5 dosimeter was used to measure neutron fluence. After irradiation, induced fission tracks in the external detectors, low U muscovite sheets, were exposed through etching in 40% HF at 21°C for 45 min. AFT ages were calculated using the external-detector and the ζ-calibration methods (Hurford and Green, 1983) with IUGS standards (Durango and Fish Canyon) and a value of 0.5 for the 4p/2p geometry correction factor. The analyses were subjected to the χ^2 test (Galbraith, 1981) to detect whether the data sets contained any extra-Poissonian age scatter. A χ^2 probability of 5% denotes that the age distribution contains multiple age populations. AFT age distributions can be decomposed into age populations using kernel density estimate techniques: we used Binomfit by Brandon (1996) that is most suitable to deal with AFT samples with low density of spontaneous tracks.

U-Pb Zircon Chronology

U-Pb isotope intensities from 431 laser ablation spots in 371 zircon crystals were measured by inductively coupled plasma mass-spectrometry (LA-ICPMS) at ETH Zurich. The ablation areas with a spot diameter of 20 μm were pre-selected with the aid of cathodoluminescence images in order to identify zonations and crystal defects, which were then avoided. Both the core and rim of zircons were measured in the suitable grains.

U and Pb were analyzed using a Resonetic Resolution 155 laser ablation system with a repetition rate of 5 Hz and an energy density of 2 J cm^{-2} coupled to a Thermo Element XR Sector-field ICP-MS measuring ^{202}Hg, ^{204}Pb, ^{206}Pb, ^{207}Pb, ^{208}Pb, ^{232}Th, ^{235}U, and ^{238}U intensities (Guillong et al., 2014). GJ-1 (Jackson et al., 2004) was used as primary reference material, and accuracy of the method was confirmed by four secondary standards (AUSZ7-5, OD-3, Temora2, and 91,500). Ages and ratios corrected for instrumental drift and down hole fractionation were obtained using the iolite 2.5 (Paton et al., 2010) and VizualAge software (Petrus and Kamber, 2012). No common Pb correction was applied, since contaminated signals are recognized as discordant ages in the Concordia plots, which were produced with Isoplot 4.1 (Ludwig, 2001). Error ellipses represent 2 s analytical errors of the $^{207}Pb/^{235}U$ and $^{206}Pb/^{238}U$ ratios, respectively.

RESULTS

Grainsize, Petrography and Composition

The sampled sediment from Raponzolo Cave is a fine (51.6%) to very fine (22.8%) sand with moderate mud (clay + silt) fraction (18.2%); the carbonate cement and very few carbonatic grains, before dissolution, accounted for 54.4% of the original weight (**Figure 5**). Thin section analyses have shown the presence of both monomineralic and polymineralic grains as following (**Figure 6**; abundant: widespread in all observations; common: present in all observations; rare: only few grains detected):

- Biotite (abundant) in form of elongated grains with rounded tips casually oriented within the sample.
- Quartz (abundant) mainly rounded or sub-rounded
- Plagioclase (common), mainly rounded and a few sub-angular grains, some with polysynthetic lamination
- Zircon, mainly fractured (common)
- K-Feldspar (rare)
- Amphibole, green hornblende (rare)
- Chalcedony (rare)
- Apatite (rare)
- Garnet (very rare)
- Kyanite (very rare)

In addition, a few polymineralic grains are representative of amphibolites, micaschists and gneiss. XRD analysis confirms thin section observations, although it was not able to define the specific amphibole as hornblende due to low lines at the limit of detection for these minerals. The composition of the sample obtained through XRF is reported in **Table 1**. High Ca content (~34%) is related to the carbonate cement, while Si from quartz and Al from silicates reach respectively 25 and 9% of the sediment, with a relatively high Fe content (2.4%) (related to biotite and iron hidroxides). *p* (0.1 %wt, in form of P_2O_5) and Zr (84 ppm) are due to the presence of apatites and zircons. Sub-rounded quartz grains are indication of transport by saltation and traction. Some of these grains show striking rounded morphologies, suggesting recycling through different erosion and transport phases. On the other hand, biotite is abundant and well preserved, with some rounded elongated morphologies related to limited transport by flotation (Garzanti et al., 2011).

Burial Time From Cosmogenic Isotopes

The $^{10}Be/^{9}Be$ ratio is very small (7.8×10^{-15}), but in line with the relatively low amount of pure quartz dissolved. Nonetheless, the

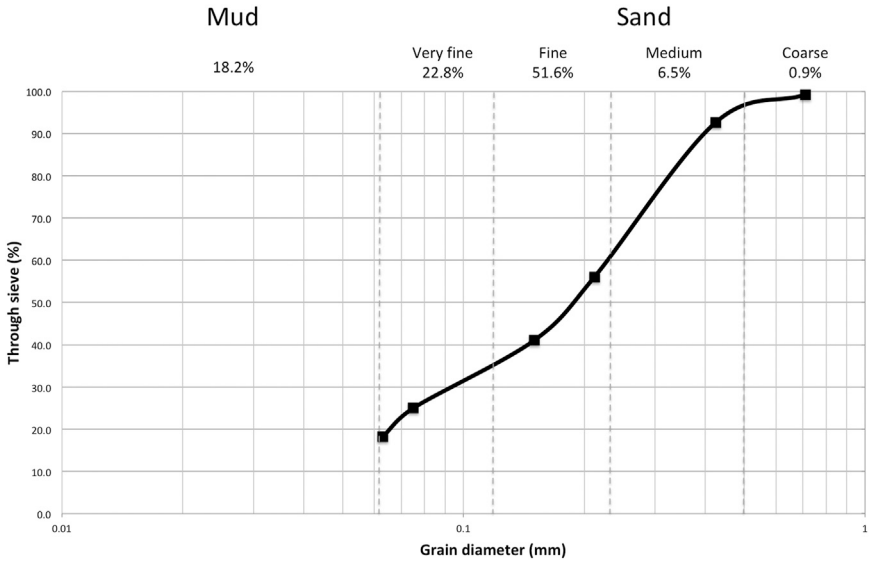

FIGURE 5 | Grainsize of the siliciclastic component of the samples: sand-size grains account for a total 81.8% while mud reached 18.2%. The siliciclastic component account for 46% of the total sample, while the total carbonate fraction (cement and few clasts) dissolved with acetic acid solution was 54% of the total sample.

error of 10% can be considered acceptable for such low values. The measurement of the procedural blanks yielded a $^{10}Be/^{9}Be$ ratio of 3.78×10^{-15} and a $^{26}Al/^{27}Al$ ratio of 6.41×10^{-15}. The blanks thus show that the measurements were good and the standards clean. All results were normalized for a ^{10}Be half-life of 1.39 Ma (Chmeleff et al., 2010; Korschinek et al., 2010). The uncertainties represent the analytical error only. The measurement of $^{26}Al/^{27}Al$ yielded a value (2.78×10^{-15}) below that of the blank (6.41×10^{-15}). Therefore, there is no detectable ^{26}Al in the sample. The combined absence of ^{26}Al and presence of ^{10}Be demonstrates that the sediment was indeed once at the surface, but that the burial time was so long that all ^{26}Al decayed because of its shorter mean half-life. Since ^{26}Al is unavailable, the exact age of the sample cannot be given, as the initial concentration of isotopes prior to burial cannot be recalculated. Nonetheless, we can infer a range of possible burial ages based on the expected mean lifetime of the sediment at the surface and isotope production rate at the altitude of the original catchment area. This hypothesis is presented in the discussion (chapter 4.2).

Paleogeographic Provenance Inferred From AFT Thermochronology and Zircon U-Pb Ages

AFT analyses (**Supplementary Table S1**) shows a distribution of dates between 4.5 ± 2.6 Ma and 56 ± 17 Ma (1σ). Two distinct populations can be identified through standard kernel density estimate techniques (Binomfit by Brandon, 1996; **Supplementary Table S2**): a minor and younger populations (P1) that includes 28% of the grains and centers at 17.6 (−2,3 + 2.6) Ma and a larger and older one (P2) that includes 72% of the grains and cetners at 23.3 Ma (−3.3 + 3.9) (**Figure 7**; **Supplementary Table S2**). The 431 U-Pb dates (**Supplementary Table S3**) show dates between 30 and >1,000 Ma old, including only two dates older than 1,000 Ma. This wide distribution consists of two main populations, a larger one (91 ± 1%) with dates centered around 35 Ma and a minor one between 270 and 600 Ma (**Figure 8**). While the first group is directly related to the emplacement of the Adamello batholith, the second is related to zircons from pre-alpine metamorphic rocks such as those of the Tonale Unit and south alpine basement, and/or to igneous zircons of the Adamello batholith with inherited cores.

DISCUSSION

Sediment Source

The petrographic composition of the sediment indicates a source situated mainly in the granitoid bodies of the Adamello Massif and in the metamorphic units of Tonale. Chalcedony is mostly related to the erosion of pseudotachylitic zones in Adamello-Presanella (Pennacchioni et al., 2006) and minor cherts eroded from the carbonatic sequence of Brenta. Metamorphic clasts (amphibolite) and minerals (especially kyanite) indicate a provenance from the Tonale Unit, which is characterized by high-P mineral suites (Davide et al., 2000).

AFT analysis provides additional indications on the source region (**Figure 9**). In the Tonale Unit, AFT dates vary between 6 and 25 Ma, and in the Adamello batholith between 8.3 and 23 Ma (Martin et al., 1998; Viola et al., 2003; Reverman et al., 2012). In both regions, AFT dates generally increase with elevation; although the AFT age-elevation relationships vary in age range and slope in different localities and in a few places they are

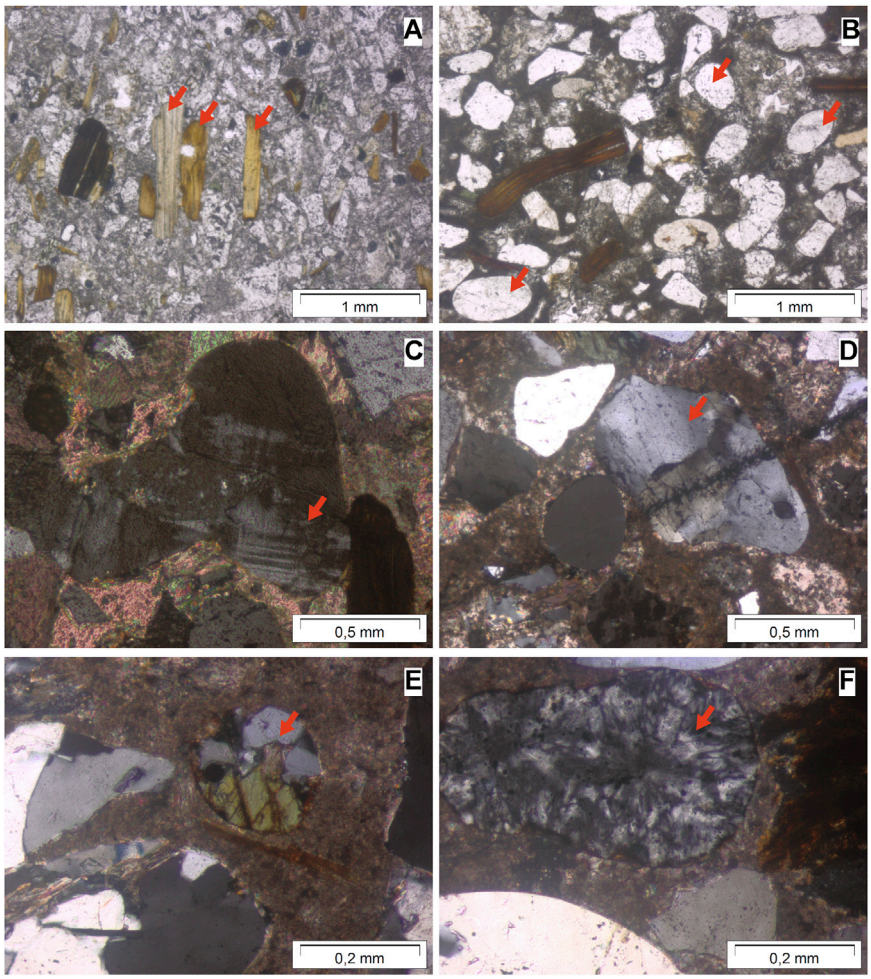

FIGURE 6 | Thin sections microphotographs [under polarizing microscope, **(A,B)** parallel polars, **(C–F)** crossed polars] showing (red arrows): **(A)** elongated biotite; **(B)** rounded to subrounded quartz; **(C)** rounded K-feldspar; **(D)** subrounded plagioclase; **(E)** a lithic grain of amphibolite (quartz + amphibole); **(F)** rounded chalcedony.

TABLE 1 | XRF results. Major elements are reported in weight percentage (%wt), Zr is reported in ppm. Other elements are considered irrelevant for this study, and thus omitted. LOI stands for loss of ignition.

Al_2O_3	CaO	Fe_2O_3	K_2O	MgO	MnO	Na_2O	P_2O_5	SiO_2	TiO_2	LOI	Zr
(wt%)	(wt%)	(wt%)	(wt%)	(wt%)	(wt%)	(wt%)	(wt%)	(wt%)	(wt%)	%	(ppm)
9.44	34.47	2.40	0.84	1.87	0.11	0.22	0.10	25.02	0.27	25.26	84

disturbed by tectonic displacements. In the sediments from Raponzolo Cave, the largest fraction (72%) of the detrital AFT dates centers at 23.3 Ma and the remaining fraction (28%) at 17.6 Ma. Thus, the largest fraction of the detrital apatites (red area in **Figure 9**) comes from the highest portions of the Tonale Unit and/or Adamello complex, at elevations above 2,300 m a.s.l, at present time. Regarding the smaller fraction at 17.6 Ma (blue area in **Figure 9**), while for Tonale the altitude range of the source region is also above the present elevation of 2,300 m a.s.l., for Adamello it is more difficult to constrain the altitude limit due to different profile distributions depending on the transect location (**Figure 9**). To solve this uncertainty, another indication is provided by zircon U-Pb ages. Zircon U-Pb ages are related to the crystallization of the magma source, which is not synchronous in all areas of the Adamello. It is thus possible to better understand which part of the batholith the sediment was eroded from if specific age groups are dominant in the cave sediment. While the older zircon age group (**Figure 9**) is related to recycling of crystals from the Permian basement and crustal rocks within the batholith (Hansmann and Oberli, 1991), the younger peak at 35 Ma indicates that the sediment source was mainly situated in the northern sectors of the Adamello batholith

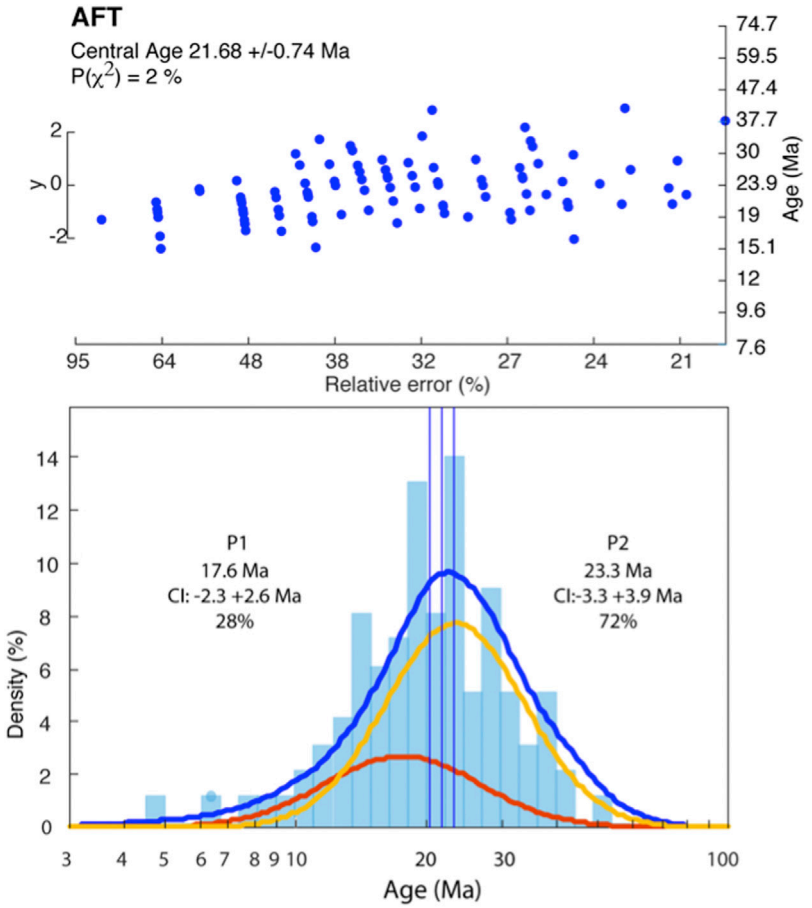

FIGURE 7 | Apatite Fission Track dating distribution in the sample. The central age of the whole population is 21.68 ± 0.74 Ma, which can be decomposed into two age populations (histogram below) using kernel density estimate techniques, showing a major peak (P2, 72%) at 23.3 Ma and a minor one (P1; 28%) at 17.6 Ma.

(Adamello North, Genova Valley, **Figures 9**, **10**), as shown by previous U-Pb, K-Ar, and Rb/Sr dating from different areas (Del Moro et al., 1983; Schaltegger et al., 2019). Very few zircons in the dataset (<10) are between 40–42 Ma indicating a negligible contribution from the southern area of the batholith (Daone, Rendena Valley; **Figures 9**, **10**; Schoene et al., 2012). This information allows to define the source region of the sediment in the northern sector of Adamello where AFT ages around 17.6 are also above 2,200–2,300 m a.s.l. at present time.

Therefore, the erosional phase producing the sediment filling Raponzolo cave occurred when the present valley network was not as deeply entrenched as today, and younger thermochronological units where not yet exposed in the source region.

Hypotheses on Age Based on Cosmogenic Nuclides

Due to the lack of ^{26}Al in the sediment, the exact age of burial cannot be calculated. However, it is possible to estimate a minimum age on the basis of the expected residence time at the surface and the cosmogenic production rate, which depends on the original altitude of the catchment area. The longer the sediment is at or near the surface (i.e., the smaller the erosion rate is), the more cosmogenic isotopes are produced. Once washed underground, these isotopes decay. If the sediment remained at the surface for a very short time, a little amount of isotopes is produced; it follows that after a comparable short burial time, the Al content would be no more measurable. The longer the sediment stayed at the surface, the more burial time is needed in order to completely deplete ^{26}Al. Therefore, in the case of the Raponzolo sediment, the main question is what a meaningful residence time at the surface could be. In order to provide a reasonable hypothesis on the residence time, we can consider the largest dataset available in the Alps: the data from Siebenhengste (Häuselmann et al., 2007). This dataset can be used as a reference for Raponzolo because of the similar settings, being Siebenhengste a karst system located within the higher ranges of the Alps (around 2000 m a.s.l.) in an area which experienced glaciations, as is the case of the Brenta Dolomites. In Siebenhengste cosmogenic dating provided erosion rates ranging from 23 to 470 m/Ma, while all but two have rates

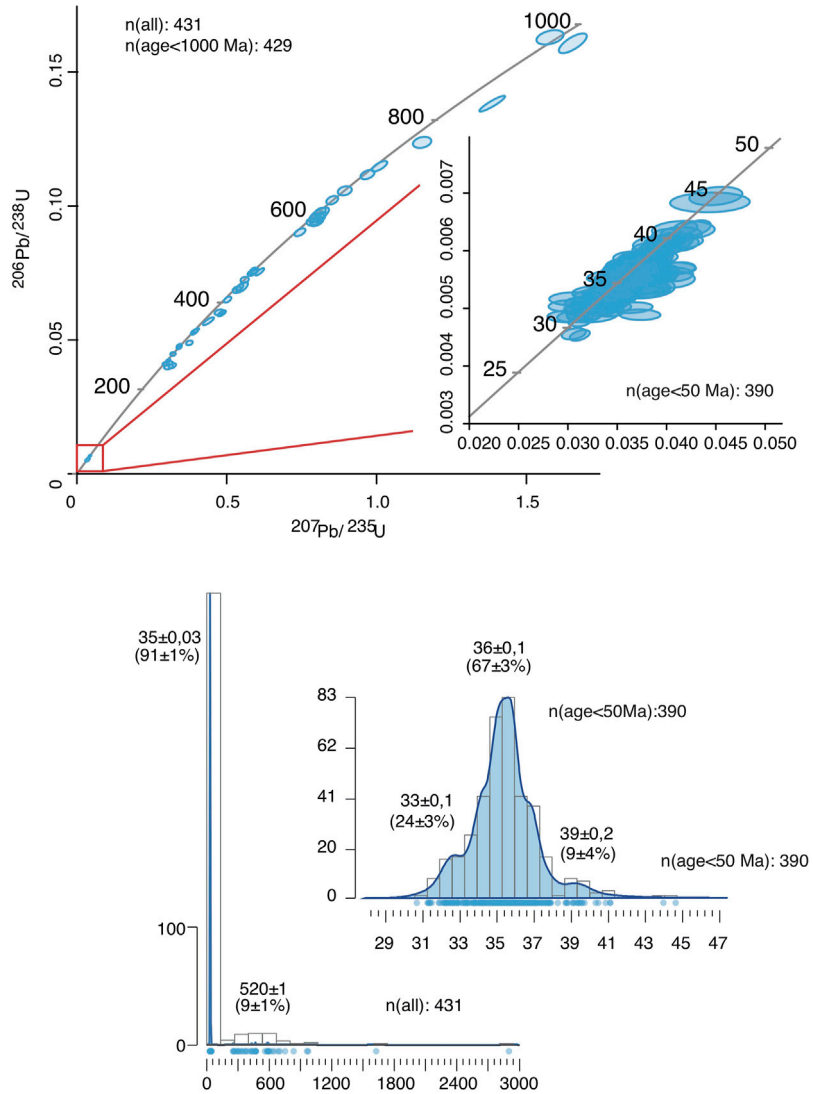

FIGURE 8 | Concordia and isochron diagrams for U-Pb dating of zircons (above). Ellipses (correlated errors) correspond to two sigma -STERR of the mean ratios. Linear regression calculations were performed with ISOPLOT-3 (Ludwig, 2001). Distribution of ages in the last 50 Ma show a peak at 36 Ma (below).

<150 m/Ma, indicating slower (pre- or interglacial) erosion. An averaged value yields 67 m/Ma, which translates into an inherited ^{10}Be amount prior to burial of 169,000 at/g. Divided by the estimated production rate in that area of 18.09 at/g/a, this gives 9,300 years residence time at the surface. The fastest, probably glacial, erosion rate gives a residence time of 1,300 years.

Since production rate is dependent on altitude, the model should also consider the approximate height of the original catchment area of the Raponzolo sediment. In order to model altitudes, production rates and erosion rates, we can use as prerequisites the available data: 1) the amount of ^{10}Be remaining in the sample measured to be 8,800 at/g; 2) no measurable ^{26}Al is present due to its complete decay. The lack of ^{26}Al can be fixed to be less than 5,000 at/g, twice the value of the blank. Considering these values, it is possible to create a model and back-calculate catchment altitudes and ages (**Supplementary Table S4**). This model shows that the fast erosion rate (surface residence time of 1,300 years) can be excluded (red ages in **Supplementary Table S4**) since it would give consistently measurable amounts of ^{26}Al (>10,000 at/g) in the sample. Therefore, we hitherto used the mean erosion rate of 67 m/Ma in the model (**Figure 10**). With this erosion rate, the model provides the minimum elevation of the catchment area (which is 1,200 m a.s.l.) and the minimum age that fulfills all prerequisites (around 5.25 Ma) (**Figure 10**). However, it is important to consider that this model output is based on the assumption that in Adamello and Brenta erosion and uplift were constant in time and space at the million-year timescale neglecting the effect of local differences as for instance fault displacement and differences in rock erodibility. This assumption is supported by

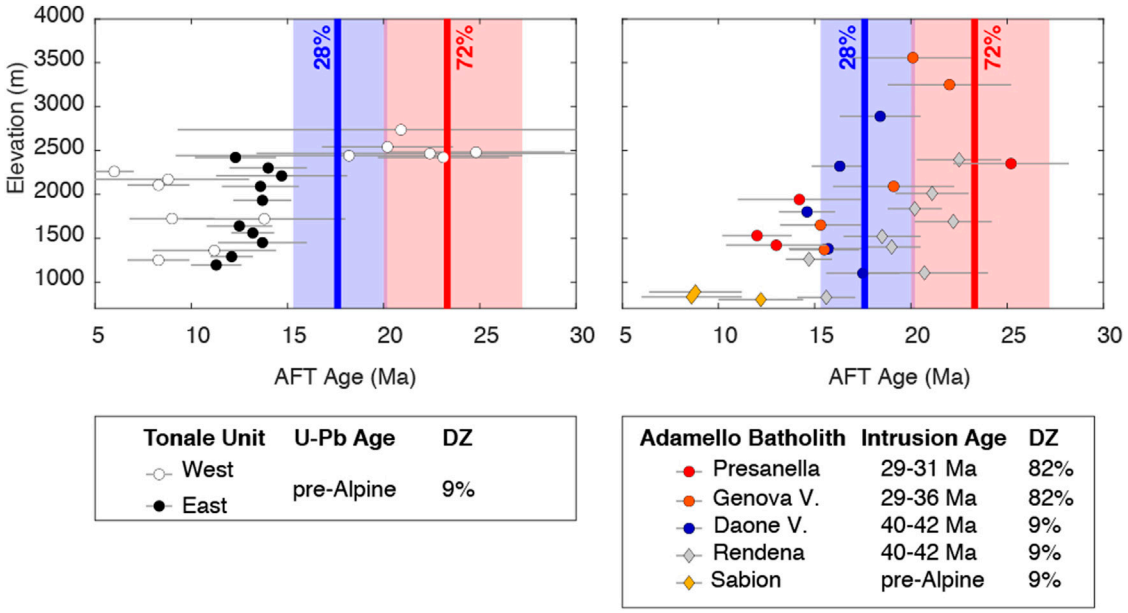

FIGURE 9 | Different AFT Age/Altitude profiles compared with the two AFT populations detected in the sediment of Raponzolo Cave (blue 17.6 Ma, red 23.3 Ma). In the lower boxes, each transect is correlated with the U-Pb age of zircons in each area. DZ shows to which percentage of ages the populations in the Raponzolo sample are associated: ages between 29 and 36 Ma (82%), ages between 40–42 (9%), pre-Alpine ages (9%). AFT profiles: Tonale from Martin et al. (1998); Presanella from Viola et al. (2001); Genova and Daone valleys from Reverman et al. (2012); Rendena from Martin et al. (1998).

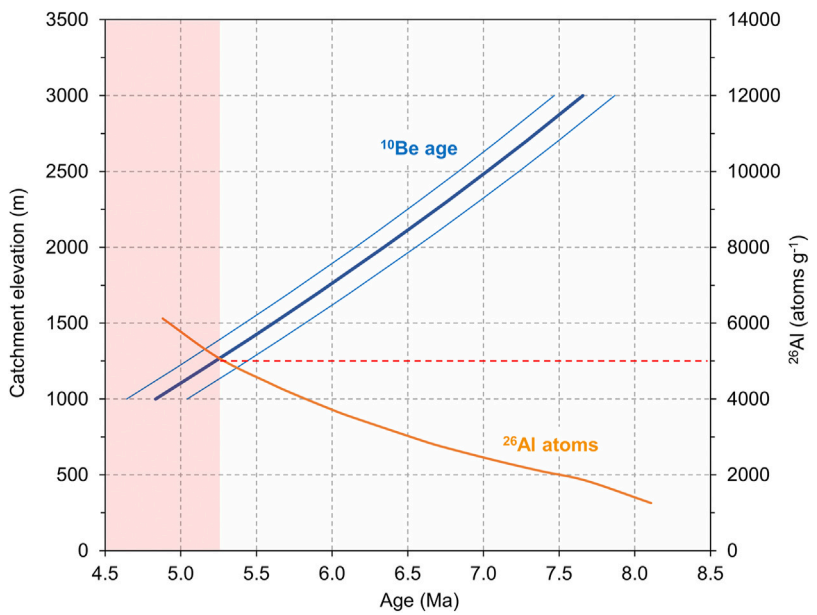

FIGURE 10 | Graph plotting the ^{10}Be burial ages as a function of the catchment elevation based on a surface sediment exposure time of 9,300 ± 930 years coupled with the calculated remaining ^{26}Al. The red dashed line at 5,000 ^{26}Al atoms/g defines the "exclusion zone" based on the absence of ^{26}Al in the sample. The line crosses the ^{10}Be age line at 5.25 Ma corresponding to a minimum catchment elevation of 1,250 m a.s.l.

thermochronologic data that in Adamello and Brenta do not resolve changes in the rate of exhumation after 4 Ma (Revermann et al., 2012) and that indicate possibly only little differential exhumation between the two massifs since 10 Ma (Heberer et al., 2017). Thus, our model points to the hypothesis that burial in the cave happened before 5.25 Ma.

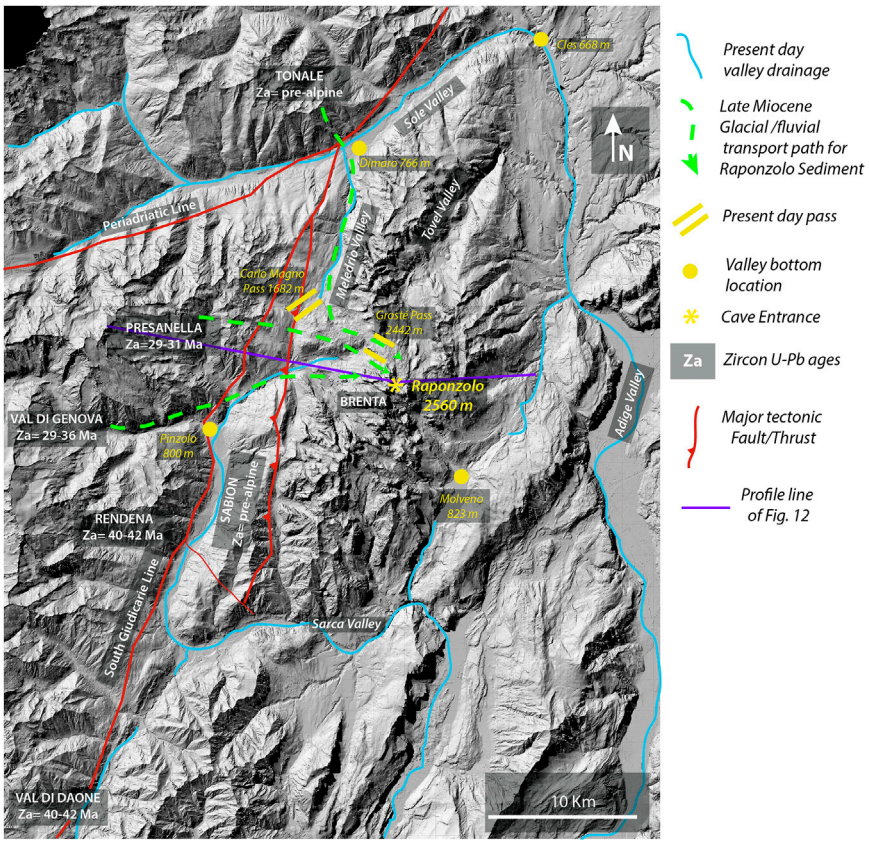

FIGURE 11 | Interpretation of sediment transport path from Adamello/Tonale toward Raponzolo Cave with the present hydrological network, major tectonic lines and U-Pb zircon ages from the different sectors.

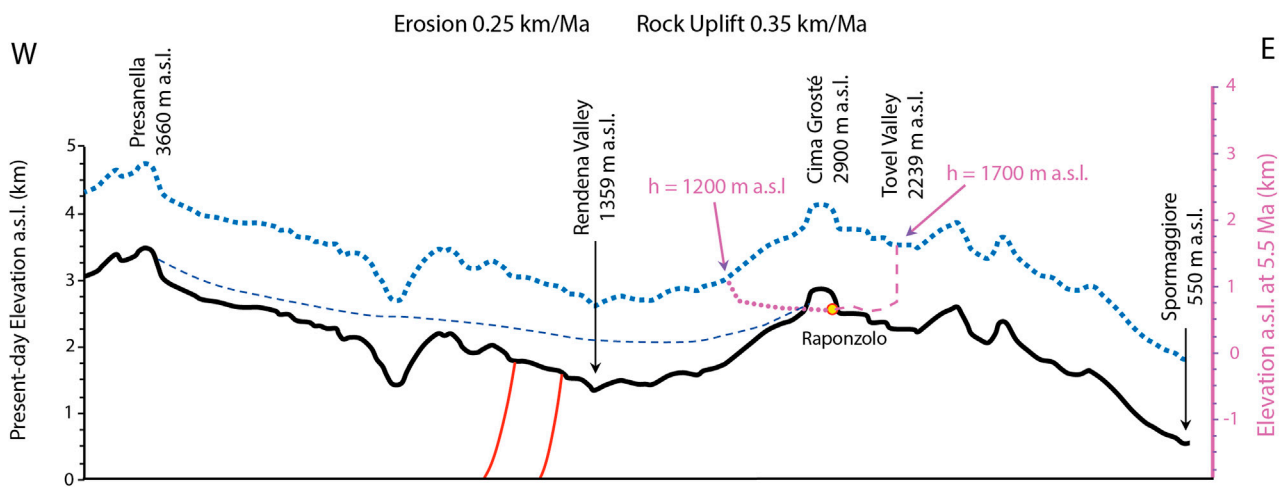

FIGURE 12 | West-east profile across the Adamello and Brenta massifs with the theoretical reconstruction of the relief at 5.5 Ma (dotted blue line). For simplicity the relief projection is based on a theoretical constant and uniform erosion rate of 0.25 km/Ma and rock uplift rate of 0.35 km/Ma, even if erosion and uplift have been surely acting with slightly different rates depending on lithologies and tectonic domains. This reconstruction is based on the assumption that nowadays valleys and prominent reliefs should have been following the footprint of the Messinian major base level drop during the Mediterranean salinity, similarly to other regions of the Alps (Garzanti and Malusà, 2008). The theoretical vertical profiles of the Raponzolo cave are represented by bold purple line (catchment in the upper Tovel valley) and dotted purple line (catchment in the Rendena valley). The dashed blue line represents the ice extent in the Rendena Valley during the Last Glacial Maximum (Trevisan, 1939).

Hints of Late Miocene Glaciations and Recycling of Fluvial Sediments

The Raponzolo Cave presents morphologies consistent with a phreatic and/or epi-phreatic origin (**Figure 3B**). The cave is probably only a fragment of an ancient karst system that has been eroded and uplifted to its present altitude (2,560 m a.s.l.). The conduits originally formed close to the water table level, which could have been situated at the level of the late Miocene valley bottom. The catchment area was situated in the northern part of the Adamello batholith up to the Tonale Unit to the north of the Periadriatic line. At present, these areas are separated from the Tovel Valley by the Rendena and Meledrio Valleys developed along the South Giudicarie Line and culminating in the Campo Carlo Magno pass at 1,682 m (**Figure 11**). Unfortunately, the irregular layering of the granitic sediments in the cave is not diagnostic of the direction of water flow during the sediment deposition, so we cannot discern if the sediment was flushed within the karst system from the Tovel valley or from the Rendena valley. These two possibilities are represented in **Figures 11**, **12**. In the profile of **Figure 12**, the present topography is projected at theoretical altitudes during the late Miocene considering, for simplicity, a constant and uniform erosion rate of 0.25 km/Ma and rock uplift rate of 0.35 km/Ma in agreement with several studies on the evolution of this alpine region (Revermann et al., 2012; Heberer et al., 2017 and references therein). This simplified assumption does not take into account differential erosion and uplift depending on lithologies and tectonic subdomains, but allows providing a general idea of the potential paleolandscape. Indeed, the Mediterranean salinity crisis and the base level dropdown during these times should have been the footprint of the present time hydrographic network in the Adamello-Brenta region, similar to what occurred in the Lepontine dome (Garzanti and Malusà, 2008). If the sediment filled the karst system entering from the Rendena Valley, the clasts of the Tonale Unit had to be transported from the Sole Valley (766 m at present-day Dimaro) uphill along the Meledrio Valley, and across Campo Carlo Magno Pass (1,682 m at present day). If the sediments had to be transported inside the Tovel valley, they would have overcome also the Grosté Pass (2,442 m at present day, **Figure 11**). From the data available and literature it is not possible to assess the hypothesis that the Meledrio or Tovel valleys were inverted at that time, allowing an efficient fluvial sediment transport from Tonale to Brenta. However, if the present topography should generally mirror the Miocene landscape, a relief inversion of these incisions after the Messinian sea level dropdown is unlikely suggesting that an uphill sediment transport from Tonale to Brenta would have been possible only by means of glaciers. The Adamello and Brenta massifs have been strongly affected by Quaternary glaciations, and during the Last Glacial Maximum, a glacial tongue from the Sole Valley filled the Meledrio Valley and surpassed the Campo Carlo Magno Pass where the reconstructed elevation of the glacier was around 2,100 m (Trevisan, 1939; Carton and Baroni, 2017). Glaciers could have used the same transport route also during more ancient glaciations and remains the best candidates for the transport of sediments of the Tonale Unit from the Sole Valley up to the Raponzolo cave entrance. This hypothesis poses an interesting dilemma because Miocene glaciations in the Alps have never been documented. Instead, sedimentary evidence of localized latest Miocene–Early Pliocene glaciations are known from Greenland (Larsen et al., 1994) to South America (Mercer and Sutter, 1982). The North Atlantic records a major cooling episode and increase in global ice volume in the period from 6.26 to 5.5 Ma that was marked by 18 glacial-to-interglacial oscillations, with the most prominent glacial phases at 5.75 and 5.51 Ma (stages TG20 and TG12; Hodell et al., 2001). These ages are within the possible range of the sediment infilling of Raponzolo being older than the minimum cosmogenic burial ages of the sediments calculated in the cosmogenic production model presented in chapter 4.2 (**Supplementary Table S4**). Also, the expected altitude of the source between 1,200 m (Rendena Valley sink, **Figure 12**) and 1700 m (Tovel Valley sink, **Figure 12**) is in agreement with the minimum altitude catchment calculated by the model.

The modest increases in global ice volume inferred from the benthic $\delta^{18}O$ signal (Hodell et al., 2001) suggest that Late Miocene glaciations were not as widespread as the Quaternary ones. In this scenario, local Alpine glaciers were probably not able to reach the Po plain and, therefore, no glacial sediments have been preserved, aside of potential local traps like caves.

A problem for this interpretation remains the roundness and well sorting of the Raponzolo sediment, which is in contrast with a glacial origin, pointing to a fluvial or aeolian transport instead. However, the first action of glacier flows is bulldozering the sediments already present at the valley bottoms (Rossato et al., 2018), which are usually rich in fluvial components. Therefore, a recycling of fluvial sediment by glacier tongues is consistent with the grain size distribution and shape, as well as with the presence of well-preserved biotite, which has not been weathered after burial (Petersen and Rasmussen, 1980; Föllmi et al., 2009). However, we cannot exclude that the most rounded quartz grains could be related to recycling of aeolian sediments, which is also consistent with an arid-cold glacial environment and with the presence of silt sized grains in the Raponzolo cave sediments (Wright, 2001).

Implications for Paleogeography and Tectonic Evolution

Cosmogenic data do not constrain a definitive age of the sediment burial, but point to a minimum age of 5.25 Ma. However, it is possible to advance additional hypotheses on the paleo-landscape during cave formation and subsequent infilling. Indeed, thermochronologic data indicate that during the late Miocene, from about 8 Ma, the Adamello batholith was exhuming rapidly to near-surface depths at about 0.65 km/Ma in response to uplift induced by tectonic activity, whereas during the Plio-Pleistocene exhumation proceeded on average at a lower rate of about 0.35 km/Ma (Reverman et al., 2012). In Brenta, on the other side of the Giudicarie line, thermochronologic data from flysch sediments on the eastern foot of the massif (Ponte Pià Formation, AFT = 9–10 Ma) indicate 3 to 2 km of rock removal since 10 Ma,

which corresponds to an average exhumation rate similar in range but possibly slightly lower than the one estimated for the Adamello massif during the late Miocene (Heberer et al., 2017). Altogether, the thermochronologic data from Adamello and Brenta, and the new data gathered from Raponzolo Cave, indicate that during the late Miocene the exhumation of the two massifs was synchronous, but the pace was possibly slightly different. This means that Adamello was possibly exhuming faster than Brenta and that this evolution may have favored a potential transfer of sediments (fluvial or glacial) from Adamello-Presanella toward Brenta. A phase of uplift and exhumation might also have favored, at the same time or shortly later, a local base-level fall; accordingly, this would be a suitable scenario for the formation of an epiphreatic cave system and its infilling. Finally, the present-day elevation of Raponzolo Cave roughly corresponds to the lower limit of its sediment source in both Adamello and Tonale as indicated by the AFT ages. This suggests that the Raponzolo sediments represent a remnant uplifted late Miocene landscape including the high elevation reaches of Tonale and Adamello, and Brenta, which was probably slightly lower in elevation as it is still today as suggested by the Ponte Pia Formation AFT ages. In this paleo-landscape, the valleys separating different geological domains (Adamello, Tonale, Brenta) were likely not as deeply entrenched as today, allowing an efficient transfer of sediment from the north-west to south-east across major tectonic lineaments, partially by fluvial systems and occasionally by glaciation events. This observation is consistent with recent studies (Winterberg et al., 2020) showing that major river valleys in inner parts of the Southern Alps (i.e., Adige Valley) were not all yet deeply carved during the Messinian sea-level drawdown.

CONCLUSION

The study of the sediments discovered in Raponzolo Cave provides new hints on the geographic, tectonic and climatic evolution of the calcareous Southern Alps in the Brenta region, and its interconnection with the Adamello crystalline bodies and the Tonale metamorphic units. Even if cosmogenic dating has not been able to define a narrow age for the sediment burial, the obtained minimum age coupled with petrographic observations, AFT ages and U-Pb on zircons provided reliable information about the sediment source and transport. Our results, combined with the known evolution of Adamello, allows inferring new clues on paleogeography of the area during the late Miocene. The data obtained thorugh the detailed analysis of the cave sediment provide the following evidences:

- The sediments were eroded from the higher (>2,200 m a.s.l) elevations of Tonale and northern Adamello-Presanella;
- The lack of ^{26}Al doesn't allow determining an exact date for the sediment burial in the cave. However, our calculation considering the remaining ^{10}Be in the sample, the mean surface exposure times of sediments in the Alps and the inferred original altitude of the source during late Miocene, points to a burial older than 5.25 Ma.

Based on these line of evidence and given the known evolution of this area of the Alps, the following hypotheses should be considered for future studies:

- The sediments were transported into Raponzolo Cave possibly by a river network or through glacial transport
- If the glacial transport would be confirmed, this could have happened during late Miocene when glaciations have been recorded in other areas of world but have been possibly overlooked in the Alps;
- At the time of sediment burial into the cave, the valley bottoms were not yet deeply entrenched allowing an efficient sediment transport from Adamello-Tonale toward Brenta.

These clues open intriguing questions that could be refined by future studies, especially if other allochtonous sediments would be identified in other caves of Brenta. For example a Miocene fluvial-glacial interconnection between different areas of the Alps (Brenta-Adamello-Tonale) suggest that the Messinian Salinity Crisis sea-level drop and related accelerated fluvial erosion may not have reached the internal most elevated region of the Southern Alps (Winterberg et al., 2020).

This is a nice case study on how a cave sediment, even from a single cave, can provide data with wide implications not only for the genesis of the cave itself but also for the complex settings and evolution of the paleo-environment of the surrounding areas. Sediments can be preserved in caves while they have been completely eroded or recycled on the surface. Therefore, the study of cave sediments in complex regions of the Alps represent a promising, still under-exploited, source of information on paleo-geography and tectonic evolution.

DATA AVAILABILITY STATEMENT

The original contributions presented in the study are included in the article/**Supplementary Material**, further inquiries can be directed to the corresponding author.

AUTHOR CONTRIBUTIONS

FS conceived the project. FS and AB carried out fieldwork. FS, MF, AC, AB wrote the draft, with contributions from PH, CC and JW. AC, MF, PH and CC accomplished lab analyses.

ACKNOWLEDGMENTS

This research was possible thanks to the logistical support of Gruppo Speleologico Trentino SAT Bindesi Villazzano especially to Walter Bronzetti and Daniele Sighel. The research was financially supported by Parco Naturale Adamello Brenta Geopark: our gratitude goes to Director Cristiano Trotte, and to Vajolet Mase and Alessia Scalfi for assistance. We are grateful

to Enrico Dinelli and Valerio Funari for XRF analysis at UNIBO, and to Marcel Guillong for LA-ICP-MS U-Pb measurements and data reduction at ETH. Finally, thanks to Giulio Viola and Paolo Garofalo (UNIBO) for the access to the optical microscope laboratory, and the three reviewers for their insightful comments.

SUPPLEMENTARY MATERIAL

The Supplementary Material for this article can be found online at: https://www.frontiersin.org/articles/10.3389/feart.2021.672119/full#supplementary-material

REFERENCES

Anthony, D. M., and Granger, D. E. (2007). A New Chronology for the Age of Appalachian Erosional Surfaces Determined by Cosmogenic Nuclides in Cave Sediments. *Earth Surf. Process. Landforms* 32, 874–887. doi:10.1002/esp.1446

Audra, P., Bini, A., Gabrovšek, F., Häuselmann, P., Hobléa, F., Jeannin, P.-Y., et al. (2007). Cave and Karst Evolution in the Alps and Their Relation to Paleoclimate and Paleotopography. *Acta Carsologica* 36, 53–67. doi:10.3986/ac.v36i1.208

Audra, P., Bini, A., Gabrovšek, F., Häuselmann, P., Hobléa, F., Jeannin, P.-Y., et al. (2006). Cave Genesis in the Alps between the Miocene and Today: a Review. *zfg* 50, 153–176. doi:10.1127/zfg/50/2006/153

Balco, G., Soreghan, G. S., Sweet, D. E., Marra, K. R., and Bierman, P. R. (2013). Cosmogenic-nuclide Burial Ages for Pleistocene Sedimentary Fill in Unaweep Canyon, Colorado, USA. *Quat. Geochronol.* 18, 149–157. doi:10.1016/j.quageo.2013.02.002

Ballesteros, D., Giralt, S., García-Sansegundo, J., and Jiménez-Sánchez, M. (2019). Quaternary regional evolution based on karst cave geomorphology in Picos de Europa (Atlantic Margin of the Iberian Peninsula). *Geomorphology* 336, 133–151. doi:10.1016/j.geomorph.2019.04.002

Bella, P., Bosák, P., Braucher, R., Pruner, P., Hercman, H., Minár, J., et al. (2019). Multi-level Domica-Baradla Cave System (Slovakia, Hungary): Middle Pliocene-Pleistocene Evolution and Implications for the Denudation Chronology of the Western Carpathians. *Geomorphology* 327, 62–79. doi:10.1016/j.geomorph.2018.10.002

Bigi, G., and Carrozzo, M. T. (1992). "Structural Model of Italy," in *Consiglio Nazionale Delle Ricerche (CNR)* (Florence: Italy), 1, 500 000.

Bini, A., Borsato, A., and Ischia, N. (1991). "Morfologia Ed Evoluzione Della Grotta Cesare Battisti (La Paganella, Trento)," in *Atti IX Convegno Regionale di Speleologia del Trentino-Alto Adige (Lavis). Natura Alpina* (Trento, Italy: Museo Tridentino di Scienze Naturali) 42, 41–77.

Borsato, A. (2001). "Characterisation of a High-Altitude alpine Karst Aquifer by Means of Temperature, Conductivity and Discharge Monitoring (Centonia spring, Brenta Dolomites, N-Italy)," in Proceedings of 7th Conference on Limestone Hydrology and Fissured Media. Editor F. Zwahlen (Besançon: France: Université de Franche-Comté), 51–54.

Borsato, A. (2007). Gli acquiferi carsici delle Dolomiti di Brenta: risorse idriche e funzionamento idrogeologico. *Memorie Istituto Italiano di Speleologia II*, 49–56.

Borsato, A. (1991). "La Grotta dello Specchio: nuova cavità del complesso carsico dei Lasteri (Gruppo di Brenta, Trentino occidentale)," in *Atti IX Convegno Regionale di Speleologia del Trentino-Alto Adige (Lavis)* (Trento: Museo Tridentino di Scienze Naturali), 42, 7–25.

Borsato, A. (2012). L'abisso Freezer ai Lasteri (Gruppo di Brenta Orientale). *XV Convegno Regionale di Speleologia Del. Trentino-alto Adige* 11, 23.

Borsato, A., Quinif, Y., Bini, A., and Dublyansky, Y. (2003). Open-system alpine Speleothems: Implications for U-Series Dating and Paleoclimate Reconstructions. *Studi Trentini di Scienze Naturali, Acta Geologica* 80, 71–83.

Borsato, A., Sartorio, D., and Frisia, S. (1994). Late Triassic-Early Liassic Stratigraphic and Diagenetic Evolution of the Margin between the Trento Platform and the Lombardy basin in the Brenta Dolomites (Italy). *Museo tridentino di scienze naturali - Acta Geologica* 69, 5–35.

Brack, P. (1983). Multiple Intrusions-Examples from the Adamello Batholith (Italy) and Their Significance on the Mechanisms of Intrusion. *Memorie della Societa Geologica Italiana* 26 (1), 145–157.

Brandon, M. T. (1996). Probability Density Plot for Fission-Track Grain-Age Samples. *Radiat. Measurements* 26, 663–676. doi:10.1016/s1350-4487(97)82880-6

Callegari, E., and Brack, P. (2002). Geological Map of the Tertiary Adamello Batholith (Northern Italy): Explanatory Notes and Legend. *Memorie di Scienze Geologiche* 54, 19–49.

Calvet, M., Gunnell, Y., Braucher, R., Hez, G., Bourlès, D., Guillou, V., et al. (2015). Cave Levels as Proxies for Measuring post-orogenic Uplift: Evidence from Cosmogenic Dating of Alluvium-Filled Caves in the French Pyrenees. *Geomorphology* 246, 617–633. doi:10.1016/j.geomorph.2015.07.013

Campani, M., Mulch, A., Kempf, O., Schlunegger, F., and Mancktelow, N. (2012). Miocene Paleotopography of the Central Alps. *Earth Planet. Sci. Lett.* 337-338, 174–185. doi:10.1016/j.epsl.2012.05.017

Carrapa, B., and Di Giulio, A. (2001). The Sedimentary Record of the Exhumation of a Granitic Intrusion into a Collisional Setting: the Lower Gonfolite Group, Southern Alps, Italy. *Sediment. Geol.* 139, 217–228. doi:10.1016/s0037-0738(00)00167-6

Carton, A., and Baroni, C. (2017). The Adamello-Presanella and Brenta Massifs, Central Alps: Contrasting High-Mountain Landscapes and Landforms, in *Landscapes and Landforms of Italy*. Editors M. Soldati and M. Marchetti (Cham: Springer Nature Switzerland), 101–112. doi:10.1007/978-3-319-26194-2_8

Castellarin, A., and Cantelli, L. (2000). Neo-Alpine Evolution of the Southern Eastern Alps. *J. Geodynamics* 30, 251–274. doi:10.1016/s0264-3707(99)00036-8

Chmeleff, J., Von Blanckenburg, F., Kossert, K., and Jakob, D. (2010). Determination of the 10Be Half-Life by Multicollector ICP-MS and Liquid Scintillation Counting. *Nucl. Instr. Methods Phys. Res. Section B: Beam Interactions Mater. Atoms* 268, 192–199. doi:10.1016/j.nimb.2009.09.012

Columbu, A., Audra, P., Gázquez, F., D'angeli, I. M., Bigot, J.-Y., Koltai, G., et al. (2021). Hypogenic Speleogenesis, Late Stage Epigenic Overprinting and Condensation-Corrosion in a Complex Cave System in Relation to Landscape Evolution (Toirano, Liguria, Italy). *Geomorphology* 376, 107561. doi:10.1016/j.geomorph.2020.107561

Columbu, A., Chiarini, V., De Waele, J., Drysdale, R., Woodhead, J., Hellstrom, J., et al. (2017). Late Quaternary Speleogenesis and Landscape Evolution in the Northern Apennine Evaporite Areas. *Earth Surf. Process. Landforms* 42, 1447–1459. doi:10.1002/esp.4099

Columbu, A., De Waele, J., Forti, P., Montagna, P., Picotti, V., Pons-Branchu, E., et al. (2015). Gypsum Caves as Indicators of Climate-Driven River Incision and Aggradation in a Rapidly Uplifting Region. *Geology* 43, 539–542. doi:10.1130/g36595.1

Columbu, A., Sauro, F., Lundberg, J., Drysdale, R., and De Waele, J. (2018). Palaeoenvironmental Changes Recorded by Speleothems of the Southern Alps (Piani Eterni, Belluno, Italy) during Four Interglacial to Glacial Climate Transitions. *Quat. Sci. Rev.* 197, 319–335. doi:10.1016/j.quascirev.2018.08.006

Conci, C., and Galvagni, A. (1952). La Grotta del Torrione di Vallesinella nel Gruppo di Brenta. *Studi Trent. Sci. Nat.*, 1–2.

Davide, G., Gosso, G., Pulcrano, E., and Iole Spalla, M. (2000). Eo-Alpine HP Metamorphism in the Permian Intrusives from the Steep belt of the central Alps (Languard-Campo Nappe and Tonale Series). *Geodinamica Acta* 13, 149–167. doi:10.1080/09853111.2000.11105370

De Waele, J., Ferrarese, F., Granger, D. E., and Sauro, F. (2012). Landscape Evolution in the Tacchi Area (central-east Sardinia, Italy) Based on Karst and Fluvial Morphology and Age of Cave Sediments. *Geografia Fisica e Dinamica Quaternaria* 35, 119–127. doi:10.4461/GFDQ.2012.35.11

Del Moro, A., Pardini, G., Quercioli, C., Villa, I., and Callegari, E. (1983). Rb/Sr and K/Ar Chronology of Adamello Granitoids, Southern Alps. *Memorie della Società Geologica Italiana* 26, 285–299.

Doglioni, C., and Bosellini, A. (1987). Eoalpine and Mesoalpine Tectonics in the Southern Alps. *Geol. Rundsch* 76, 735–754. doi:10.1007/bf01821061

Fairchild, I. J., Smith, C. L., Baker, A., Fuller, L., Spötl, C., Mattey, D., et al. (2006). Modification and Preservation of Environmental Signals in Speleothems. *Earth-Science Rev.* 75, 105–153. doi:10.1016/j.earscirev.2005.08.003

Fellin, M. G., Martin, S., and Massironi, M. (2002). Polyphase Tertiary Fault Kinematics and Quaternary Reactivation in the central-eastern Alps (Western Trentino). *J. Geodynamics* 34, 31–46. doi:10.1016/s0264-3707(01)00072-2

Föllmi, K. B., Arn, K., Hosein, R., Adatte, T., and Steinmann, P. (2009). Biogeochemical Weathering in Sedimentary Chronosequences of the Rhône and Oberaar Glaciers (Swiss Alps): Rates and Mechanisms of Biotite Weathering. *Geoderma* 151 (3-4), 270–281. doi:10.1016/j.geoderma.2009.04.012

Fox, M., Herman, F., Willett, S. D., and Schmid, S. M. (2016). The Exhumation History of the European Alps Inferred from Linear Inversion of Thermochronometric Data. *Am. J. Sci.* 316, 505–541. doi:10.2475/06.2016.01

Galbraith, R. F. (1981). On Statistical Models for Fission Track Counts. *Math. Geology.* 13, 471–478. doi:10.1007/bf01034498

Garzanti, E., Andó, S., France-Lanord, C., Censi, P., Vignola, P., Galy, V., et al. (2011). Mineralogical and Chemical Variability of Fluvial Sediments 2. Suspended-Load silt (Ganga-Brahmaputra, Bangladesh). *Earth Planet. Sci. Lett.* 302, 107–120. doi:10.1016/j.epsl.2010.11.043

Garzanti, E., and Malusà, M. G. (2008). The Oligocene Alps: Domal Unroofing and Drainage Development during Early Orogenic Growth. *Earth Planet. Sci. Lett.* 268, 487–500. doi:10.1016/j.epsl.2008.01.039

Gosse, J. C., and Phillips, F. M. (2001). Terrestrial *In Situ* Cosmogenic Nuclides: Theory and Application. *Quat. Sci. Rev.* 20, 1475–1560. doi:10.1016/s0277-3791(00)00171-2

Granger, D. E. (2006). A Review of Burial Dating Methods Using ^{26}Al and ^{10}Be. *Spec. Papers-Geological Soc. America* 415, 1–16. doi:10.1130/2006.2415(01)

Granger, D. E., Fabel, D., and Palmer, A. N. (2001). Pliocene–Pleistocene Incision of the Green River, Kentucky, Determined from Radioactive Decay of Cosmogenic 26Al and 10Be in Mammoth Cave Sediments. *Geol. Soc. America Bull.* 113, 825–836. doi:10.1130/0016-7606(2001)113<0825:ppiotg>2.0.co;2

Granger, D. E., Gibbon, R. J., Kuman, K., Clarke, R. J., Bruxelles, L., and Caffee, M. W. (2015). New Cosmogenic Burial Ages for Sterkfontein Member 2 Australopithecus and Member 5 Oldowan. *Nature* 522, 85–88. doi:10.1038/nature14268

Guillong, M., Von Quadt, A., Sakata, S., Peytcheva, I., and Bachmann, O. (2014). LA-ICP-MS Pb-U Dating of Young Zircons from the Kos-Nisyros Volcanic centre, SE Aegean Arc. *J. Anal. Spectrom.* 29, 963–970. doi:10.1039/c4ja00009a

Hansmann, W., and Oberli, F. (1991). Zircon Inheritance in an Igneous Rock Suite from the Southern Adamello Batholith (Italian Alps). *Contr. Mineral. Petrol.* 107, 501–518. doi:10.1007/bf00310684

Häuselmann, P. (2007). How to Date Nothing with Cosmogenic Nuclides. *Acta Carsologica* 36, 93–100. doi:10.3986/ac.v36i1.212

Häuselmann, P., Fiebig, M., Kubik, P. W., and Adrian, H. (2007). A First Attempt to Date the Original "Deckenschotter" of Penck and Brückner with Cosmogenic Nuclides. *Quat. Int.* 164-165, 33–42. doi:10.1016/j.quaint.2006.12.013

Häuselmann, P., and Granger, D. E. (2005). Dating of Caves by Cosmogenic Nuclides: Method, Possibilities, and the Siebenhengste Example(Switzerland). *Acta Carsologica* 34, 43–50. doi:10.3986/ac.v34i1.278

Häuselmann, P., Mihevc, A., Pruner, P., Horáček, I., Čermák, S., Hercman, H., et al. (2015). Snežna Jama (Slovenia): Interdisciplinary Dating of Cave Sediments and Implication for Landscape Evolution. *Geomorphology* 247, 10–24. doi:10.1016/j.geomorph.2014.12.034

Häuselmann, P., Plan, L., Plan, L., Pointner, P., and Fiebig, M. (2020). Cosmogenic Nuclide Dating of Cave Sediments in the Eastern Alps and Implications for Erosion Rates. *Ijs* 49, 107–118. doi:10.5038/1827-806x.49.2.2303

Heberer, B., Reverman, R. L., Fellin, M. G., Neubauer, F., Dunkl, I., Zattin, M., et al. (2017). Postcollisional Cooling History of the Eastern and Southern Alps and its Linkage to Adria Indentation. *Int. J. Earth Sci. (Geol Rundsch)* 106, 1557–1580. doi:10.1007/s00531-016-1367-3

Hodell, D. A., Curtis, J. H., Sierro, F. J., and Raymo, M. E. (2001). Correlation of Late Miocene to Early Pliocene Sequences between the Mediterranean and North Atlantic. *Paleoceanography* 16, 164–178. doi:10.1029/1999pa000487

Hurford, A. J., and Green, P. F. (1983). The Zeta Age Calibration of Fission-Track Dating. *Chem. Geology.* 41, 285–317. doi:10.1016/s0009-2541(83)80026-6

Jackson, S. E., Pearson, N. J., Griffin, W. L., and Belousova, E. A. (2004). The Application of Laser Ablation-Inductively Coupled Plasma-Mass Spectrometry to *In Situ* U-Pb Zircon Geochronology. *Chem. Geology.* 211, 47–69. doi:10.1016/j.chemgeo.2004.06.017

Korschinek, G., Bergmaier, A., Faestermann, T., Gerstmann, U. C., Knie, K., Rugel, G., et al. (2010). A New Value for the Half-Life of 10Be by Heavy-Ion Elastic Recoil Detection and Liquid Scintillation Counting. *Nucl. Instr. Methods Phys. Res. Section B: Beam Interactions Mater. Atoms* 268, 187–191. doi:10.1016/j.nimb.2009.09.020

Kuhlemann, J., and Kempf, O. (2002). Post-eocene Evolution of the North Alpine Foreland Basin and its Response to Alpine Tectonics. *Sediment. Geology.* 152, 45–78. doi:10.1016/s0037-0738(01)00285-8

Larsen, H. C., Saunders, A. D., Clift, P. D., Beget, J., Wei, W., and Spezzaferri, S. (1994). Seven Million Years of Glaciation in Greenland. *Science* 264, 952–955. doi:10.1126/science.264.5161.952

Ludwig, K. (2001). *A Geochronological Tool Kit for Microsoft Excel*. Berkeley Geochronology Center, 55. Isoplot/Ex rev. 2.49.

Malusà, M. G., Zattin, M., Andò, S., Garzanti, E., and Vezzoli, G. (2009). Focused Erosion in the Alps Constrained by Fission-Track Ages on Detrital Apatites. *Geol. Soc. Lond. Spec. Publications* 324 (1), 141–152. doi:10.1144/sp324.11

Martin, S., Bigazzi, G., Zattin, M., Viola, G., and Balestrieri, M. L. (1998). Neogene Kinematics of the Giudicarie Fault (Central-Eastern Alps, Italy): New Apatite Fission-track Data. *Terra Nova* 10, 217–221. doi:10.1046/j.1365-3121.1998.00119.x

Martin, S., Prosser, G., and Morten, L. (1993). Tectono-magmatic Evolution of Sheeted Plutonic Bodies along the north Giudicarie Line (Northern Italy). *Geol. Rundsch* 82, 51–66. doi:10.1007/bf00563270

Mercer, J. H., and Sutter, J. F. (1982). Late Miocene-Earliest Pliocene Glaciation in Southern Argentina: Implications for Global Ice-Sheet History. *Palaeogeogr. Palaeoclimatol. Palaeoecol.* 38, 185–206. doi:10.1016/0031-0182(82)90003-7

Naeser, C. W. (1979). Fission-track Dating and Geologic Annealing of Fission Tracks," in *Lectures in Isotope Geology*. Editor E. Jäger (Heidelberg: Springer), 154–169. doi:10.1007/978-3-642-67161-6_10

Nicod, J. (1976). Les Dolomites de la Brenta (Italie) Karst haut-alpin typique et le problème des cuvettes glacio-karstiques. *Z. für Geomorphologie Suppl. Band* 26, 35–57.

Nishiizumi, K., Winterer, E. L., Kohl, C. P., Klein, J., Middleton, R., Lal, D., et al. (1989). Cosmic ray Production Rates of10Be and26Al in Quartz from Glacially Polished Rocks. *J. Geophys. Res.* 94, 17907–17915. doi:10.1029/jb094ib12p17907

Paton, C., Woodhead, J. D., Hellstrom, J. C., Hergt, J. M., Greig, A., and Maas, R. (2010). Improved Laser Ablation U-Pb Zircon Geochronology through Robust Downhole Fractionation Correction. *Geochem. Geophys. Geosystems* 11, 1–36. 10.1029/2009GC002618. Art. Q0AA06.

Pennacchioni, G., Di Toro, G., Brack, P., Menegon, L., and Villa, I. M. (2006). Brittle-ductile-brittle Deformation during Cooling of Tonalite (Adamello, Southern Italian Alps). *Tectonophysics* 427, 171–197. doi:10.1016/j.tecto.2006.05.019

Petersen, L., and Rasmussen, K. (1980). Mineralogical Composition of the clay Fraction of Two Fluvio-Glacial Sediments from East Greenland. *Clay miner.* 15 (2), 135–145. doi:10.1180/claymin.1980.015.2.04

Petrus, J. A., and Kamber, B. S. (2012). VizualAge: A Novel Approach to Laser Ablation ICP-MS U-Pb Geochronology Data Reduction. *Geostandards Geoanalytical Res.* 36, 247–270. doi:10.1111/j.1751-908x.2012.00158.x

Potter, P. E., and Szatmari, P. (2009). Global Miocene Tectonics and the Modern World. *Earth-Science Rev.* 96 (4), 279–295. doi:10.1016/j.earscirev.2009.07.003

Reverman, R. L., Fellin, M. G., Herman, F., Willett, S. D., and Fitoussi, C. (2012). Climatically versus Tectonically Forced Erosion in the Alps: Thermochronometric Constraints from the Adamello Complex, Southern Alps, Italy. *Earth Planet. Sci. Lett.* 339-340, 127–138. doi:10.1016/j.epsl.2012.04.051

Rossato, S., Carraro, A., Monegato, G., Mozzi, P., and Tateo, F. (2018). Glacial Dynamics in Pre-Alpine Narrow Valleys during the Last Glacial Maximum Inferred by lowland Fluvial Records (Northeast Italy). *Earth Surf. Dynam.* 6 (3), 809–828. doi:10.5194/esurf-6-809-2018

Sauro, F., Piccini, L., Menichetti, M., Artoni, A., and Migliorini, E. (2012). Lithological and Structural Guidance on Speleogenesis in Spluga Della Preta Cave, Lessini Mountains (Veneto-Italy). *Geogr. Fis. Din. Quat.* 35, 167–176. doi:10.4461/GFDQ.2012.35.15

Sauro, F., Zampieri, D., and Filipponi, M. (2013). Development of a Deep Karst System within a Transpressional Structure of the Dolomites in north-east Italy. *Geomorphology* 184, 51–63. doi:10.1016/j.geomorph.2012.11.014

Schaltegger, U., Nowak, A., Ulianov, A., Fisher, C. M., Gerdes, A., Spikings, R., et al. (2019). Zircon Petrochronology and 40Ar/39Ar Thermochronology of the Adamello Intrusive Suite, N. Italy: Monitoring the Growth and Decay of an Incrementally Assembled Magmatic System. *J. Pet.* 60, 701–722. doi:10.1093/petrology/egz010

Schlunegger, F., and Mosar, J. (2011). The Last Erosional Stage of the Molasse Basin and the Alps. *Int. J. Earth Sci. (Geol Rundsch)* 100, 1147–1162. doi:10.1007/s00531-010-0607-1

Schmid, S. M., Fügenschuh, B., Kissling, E., and Schuster, R. (2004). Tectonic Map and Overall Architecture of the Alpine Orogen. *Eclogae Geol. Helv.* 97, 93–117. doi:10.1007/s00015-004-1113-x

Schoene, B., Schaltegger, U., Brack, P., Latkoczy, C., Stracke, A., and Günther, D. (2012). Rates of Magma Differentiation and Emplacement in a Ballooning Pluton Recorded by U-Pb TIMS-TEA, Adamello Batholith, Italy. *Earth Planet. Sci. Lett.* 355-356, 162–173. doi:10.1016/j.epsl.2012.08.019

Spalla, M., Zucali, M., Salvi, F., Gosso, G., and Gazzola, D. (2003). Tectono-metamorphic map of the Languard-Campo-Serie del Tonale nappes between upper Val Camonica and Valtellina (Central Italian Alps, Austroalpine Domain). *Memorie di Scienze Geologiche* 55, 105–118.

Stalder, N. F., Fellin, M. G., Caracciolo, L., Guillong, M., Winkler, W., Milli, S., et al. (2018). Dispersal Pathways in the Early Messinian Adriatic Foreland and Provenance of the Laga Formation (Central Apennines, Italy). *Sediment. Geology.* 375, 289–308. doi:10.1016/j.sedgeo.2017.09.016

Stefani, C., Fellin, M. G., Zattin, M., Zuffa, G. G., Dalmonte, C., Mancin, N., et al. (2007). Provenance and Paleogeographic Evolution in a Multi-Source Foreland: The Cenozoic Venetian Friulian Basin (NE Italy). *J. Sediment. Res.* 77, 867–887. doi:10.2110/jsr.2007.083

Stipp, M., Stünitz, H., Heilbronner, R., and Schmid, S. M. (2002). The Eastern Tonale Fault Zone: a 'natural Laboratory' for crystal Plastic Deformation of Quartz over a Temperature Range from 250 to 700°C. *J. Struct. Geology.* 24, 1861–1884. doi:10.1016/s0191-8141(02)00035-4

Stock, G. M., Anderson, R. S., and Finkel, R. C. (2005a). Rates of Erosion and Topographic Evolution of the Sierra Nevada, California, Inferred from cosmogenic26Al and10Be Concentrations. *Earth Surf. Process. Landforms* 30, 985–1006. doi:10.1002/esp.1258

Stock, G. M., Granger, D. E., Sasowsky, I. D., Anderson, R. S., and Finkel, R. C. (2005b). Comparison of U-Th, Paleomagnetism, and Cosmogenic Burial Methods for Dating Caves: Implications for Landscape Evolution Studies. *Earth Planet. Sci. Lett.* 236, 388–403. doi:10.1016/j.epsl.2005.04.024

Trevisan, L. (1939). *Il Gruppo di Brenta:(Trentino occidentale)*. Roma: Società Cooperativa Tipografica.

Viola, G., Mancktelow, N. S., and Seward, D. (2001). Late Oligocene-Neogene Evolution of Europe-Adria Collision: New Structural and Geochronological Evidence from the Giudicarie Fault System (Italian Eastern Alps). *Tectonics* 20, 999–1020. doi:10.1029/2001tc900021

Viola, G., Mancktelow, N. S., Seward, D., Meier, A., and Martin, S. (2003). The Pejo Fault System: an Example of Multiple Tectonic Activity in the Italian Eastern Alps. *Geol. Soc. America Bull.* 115, 515–532. doi:10.1130/0016-7606(2003)115<0515:tpfsae>2.0.co;2

Winterberg, S., Picotti, V., and Willett, S. D. (2020). Messinian or Pleistocene valley Incision within the Southern Alps. *Swiss J. Geosciences* 113, 1–14. doi:10.1186/s00015-020-00361-7

Winterberg, S., and Willett, S. D. (2019). Greater Alpine River Network Evolution, Interpretations Based on Novel Drainage Analysis. *Swiss J. Geosci.* 112, 3–22. doi:10.1007/s00015-018-0332-5

Wright, J. S. (2001). Desert" Loess versus "Glacial" Loess: Quartz silt Formation, Source Areas and Sediment Pathways in the Formation of Loess Deposits. *Geomorphology* 36 (3–4), 231–256. doi:10.1016/S0169-555X(00)00060-X

Conflict of Interest: The authors declare that the research was conducted in the absence of any commercial or financial relationships that could be construed as a potential conflict of interest.